

LA-UR- 08-5943

Approved for public release;
distribution is unlimited.

Title: Visualization for materials science and nanoscience.

Author(s): M. Graf, T-11/T-Division
A. Balatsky, T-11/T-Division

Intended for: SciDAC Review



Los Alamos National Laboratory, an affirmative action/equal opportunity employer, is operated by the Los Alamos National Security, LLC for the National Nuclear Security Administration of the U.S. Department of Energy under contract DE-AC52-06NA25396. By acceptance of this article, the publisher recognizes that the U.S. Government retains a nonexclusive, royalty-free license to publish or reproduce the published form of this contribution, or to allow others to do so, for U.S. Government purposes. Los Alamos National Laboratory requests that the publisher identify this article as work performed under the auspices of the U.S. Department of Energy. Los Alamos National Laboratory strongly supports academic freedom and a researcher's right to publish; as an institution, however, the Laboratory does not endorse the viewpoint of a publication or guarantee its technical correctness.

To see is to know:

Visualization for materials science and nanoscience

Dr. Matthias J. Graf, Dr. James Ahrens, John Patchett, Nathan Brown, Dr. Hari Dahal & Dr. Alexander V. Balatsky

Los Alamos National Laboratory, Los Alamos, New Mexico 87545, USA

The Center for Integrated Nanotechnology (CINT) is a Department of Energy funded center jointly operated by Sandia National Laboratory and Los Alamos National Laboratory. As part of the Los Alamos located CINT facilities, we have developed a visualization capability hosted in the VIZ lab at CINT that is focused on using established applications and developing new visualization tools for the use in materials science and more specifically for the nanosciences. The utility of the visualization process is captured by the motto “To see is to know”, which is so ingrained in the way we do science that often we forget that it is one of the pillars of the scientific methods, namely to record or demonstrate an effect and its causal connection in a reproducible way. Visualization is one of the tools that enables scientists to convincingly demonstrate and present their results. This idea underpins the logic of many visualization facilities in the United States and elsewhere. Where visualization at CINT is unique is its focus on the nanoscience and nanoscale effects that control materials properties. In this article, we will give specific examples on how visualization helps scientists and users at the Center.

The CINT gateway at Los Alamos is applying the motto “To see is to know” to its visualization laboratory, where scientists and program users alike have access to advanced active stereo three-dimensional visualization tools. By bringing visualization tools and a stereo visualization laboratory in close proximity to scientists, CINT is empowering the individual researcher in materials science and nanoscience with unprecedented capabilities to explore complex or multi-dimensional scientific datasets. In nanoscience, materials science and condensed matter physics researchers are more and more often overwhelmed by the amount or complexity of data produced in table-top experiments or numerical computations. Our understanding of collected or calculated data is sometimes limited by the means of how well we can visualize or present it. Visualization enhances our ability to see unexpected patterns and correlations in measurements and simulations. The lack of proper visualization can be responsible for our failure to understand the true meaning of our data. This becomes especially important when dealing with a large parameter space of unknowns in experiment or theory, or when quantifying differences between datasets and images.

[sidebar 1 “What is visualization?”: Visualization is the process of creating a visual representation of scientific results in order to enhance our understanding. Two major steps are involved in visualization: 1) a visualization step, applying a visualization algorithm that creates a visual representation and 2) a rendering step, the display of this visual representation. Different algorithms can highlight different aspects of a scientific result. For example, a contouring algorithm shows the relationship between a given value in a dataset. A cut plane operation produces a plane containing the data where it intersects the dataset, the resultant plane dataset can have further visualization operations performed on it. When presenting a complex relationship in a dataset, it can be helpful to use the many visual cues, including spatial dimensions (1,2, 3 dimensions), color, depth and shading. Interactivity, the ability to quickly manipulate and dynamically explore a dataset by rotating, panning and zooming, is very useful to understand a dataset's internal structure and relationships. Rendering is the simulation of the physics of light interacting on a collection of objects. Scientific visualization algorithms create these geometric objects. It is important to provide depth cues in order to understand three dimensional datasets, objects and their structure.

In the real world, we get depth cues by having a different image come to each eye (stereoscopic viewing). These images are processed by the brain to form a three dimensional model of the scene we are viewing. A similar process is possible using stereo technology. Passive stereo techniques use static lens/filters to present a different image to each eye. An example of this is red-blue stereo, in which a user wears a pair of glasses with a red and a blue lens. When rendering, each image is a composite of a left eye image in blue and a right eye image in red. The red filter removes the red data, showing a left-eye perspective (i.e. blue image content) to the left eye. Using a blue filter, a right-eye perspective (i.e. red image content) is shown to the right eye.

Active stereo techniques use shutters that alternate showing left eye and right eye views blocking one eye from viewing while the other eye views the scene from their perspective. CINT has chosen an active stereo solution for their visualization laboratory. Fakespace Inc., installed a stereo projection system connected to a high-end graphics workstation.

Collected together, visualization and rendering algorithms form a visualization tool. There are a number of commercial and open-source visualization tools available. For CINT, we use primarily ParaView (www.paraview.org), because it offers a full suite of visualization and rendering capabilities and is freely available under an open-source license.]

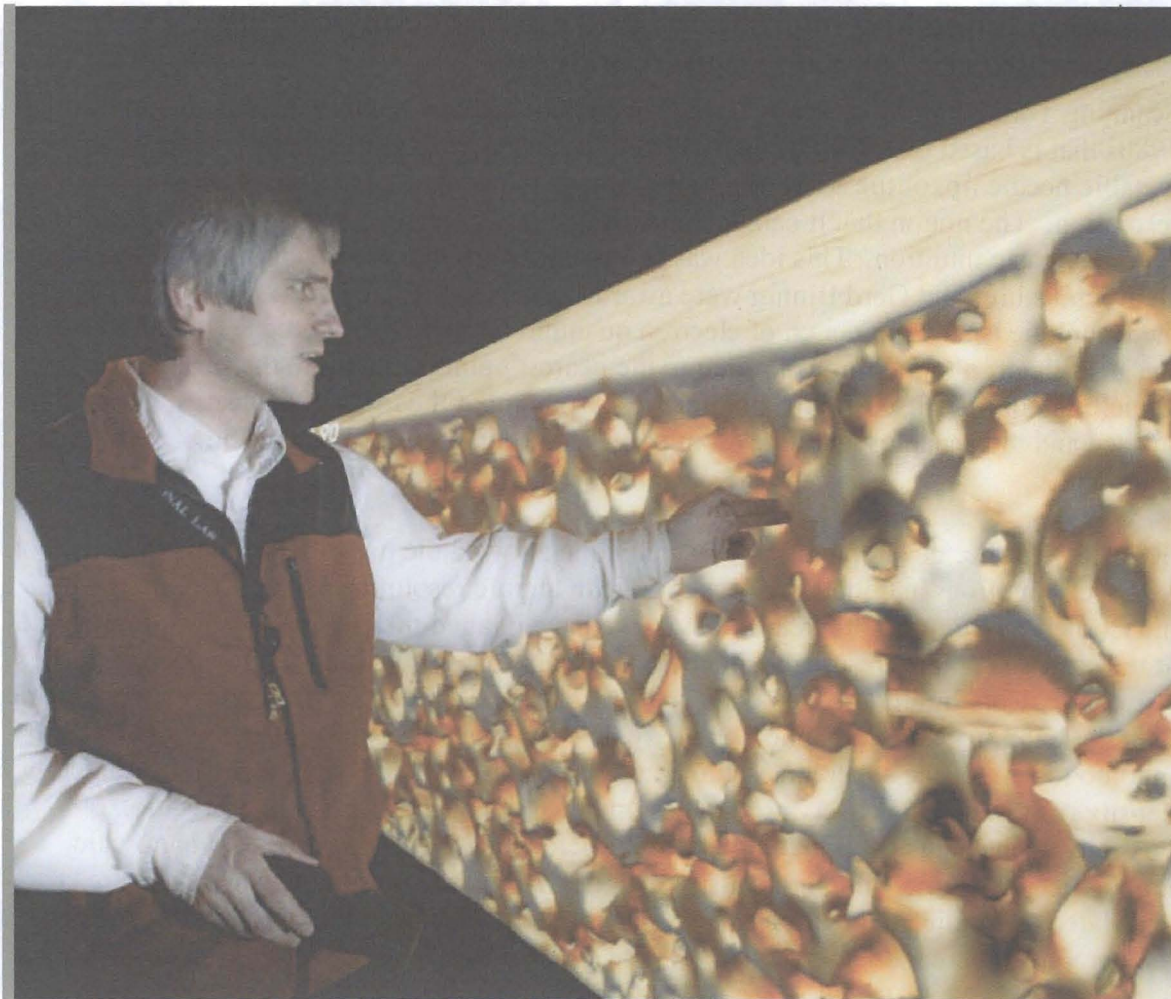


Figure caption: In the Los Alamos Center for Integrated Nanotechnologies stereo visualization laboratory, Matthias Graf explains the elastic and structural properties of a compressed foam pad simulation by Dr. Scott Bardenhagen of Physics and Chemistry of Materials group at Los Alamos. The red color indicates regions of high stress superimposed onto the foam structure. (Photo is courtesy by Robert W. Kramer)

In the rest of this article, we will highlight our collaborations with nanotechnology and condensed matter scientists to understand their acquired data through the use of visualization. A general theme from each of the examples is that complementing 2D plots with 3D visualization techniques leads to an increased understanding of the data and especially the relationships between the visualized variables and real or hyper-dimensional space.

Scanning tunnelling microscopy and spectroscopy of high-temperature copper-oxide superconductor

Scanning Tunnelling Microscopy (STM) is a relatively new technique, invented in the 1980s that is based on a revolutionary idea to use a macroscopic object, that means a metallic needle tip, of the STM as a tool to image the surface of materials with atomic resolution. The notion that it can be done using a large macroscopic object goes against our everyday basic intuition. This idea was so revolutionary that the inventors of this technique Heinrich Rohrer and Gerd Binnig were awarded the Nobel Prize in Physics in 1986. Key to the technique is a phenomenon of electron quantum tunnelling from the tip to the surface. Because electron tunnelling is limited to the nearest point of the tip to the surface the tunnelling confines itself to the atomically sharp point at the tip and the nearest point at the surface and thus enables us to see atomically sharp images with a resolution of better than 0.1 nm.

Recently, further development of this technique allowed the use of STM tunnelling as tool to detect vibrations and inelastic processes with atomic resolution. In collaboration with the Cornell STM group of Dr. J.C. Davis, we have imaged the inelastic scattering processes at the scale of 2-5 nm in superconducting materials with a transition temperature of 76 K. For comparison, liquid nitrogen boils at 77 K. We have found that indeed this copper-oxide material exhibits nanoscale inhomogeneity that correlates with the nanoscale inhomogeneity of the superconducting gap or strength of the Cooper pairs in the tunneling density of states. This observation opens up new possibilities for the interpretation of possible mechanisms for high temperature superconductivity. The observed nanoscale inhomogeneity in the tunneling density of states and in inelastic scattering modes are cross-correlated and indicate the importance of the inelastic electron scattering process in high temperature superconductors.

This experiment, along with others, supports the observation that a growing list of modern functional materials are inhomogeneous at the nanoscale. This work is part of the science efforts at CINT, which address the role that artificial nanoscale structures or intrinsic nanoscale inhomogeneities play in the function of modern materials.

The cover figure shows processed data from an STM experiment in real space of the high-temperature copper-oxide superconductor $\text{Bi}_2\text{Sr}_2\text{CaCu}_2\text{O}_{8+\delta}$ with a transition temperature of $T_c=76$ K. The image is the 3D map of the inelastic mode Ω , which provides a visualization of the putative pairing glue of Cooper pairs in the above-mentioned high- T_c superconductor. In the theory of superconductivity, for which John Bardeen, Leon Cooper and Robert Schrieffer received the Nobel Prize of Physics in 1972, it is known that below the superconducting transition temperature it is energetically favorable for electrons to form pairs with a macroscopic quantum coherence that results in dissipationless conductivity. In the figure of the cover page Ω is plotted as function of the two-dimensional momentum space coordinates (k_x, k_y) . The Ω map is recorded as function of the external voltage bias between tunneling tip and sample and plotted along the vertical axis.

The phase diagram of heavy-fermion superconductor CeRhIn₅

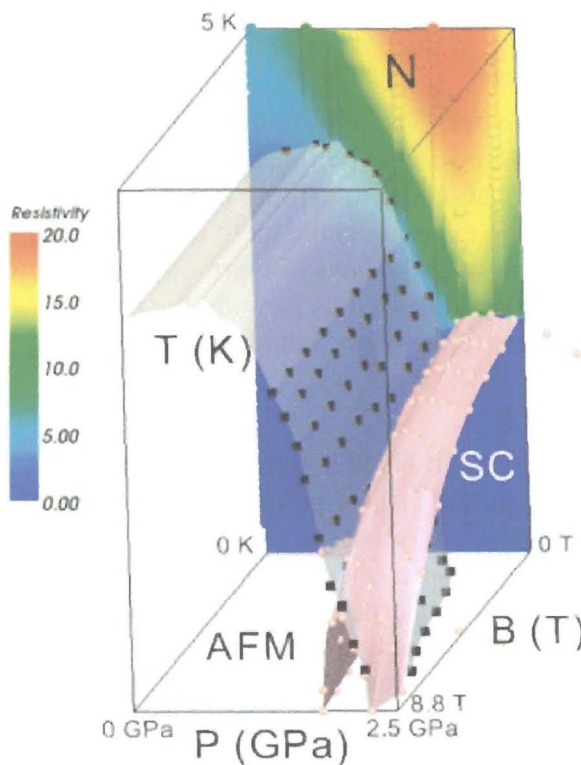
Phases of matter in thermodynamic equilibrium are best described using a phase diagram. Each phase exhibits unique physical characteristics and a phase diagram, traditionally drawn in 2D, shows where transitions between phases will occur based on various types of external variables like pressure, temperature and magnetic field. In collaboration with Dr. Tuson Park and Dr. Joe Thompson at Los Alamos National Laboratory we have worked on visualizing the phase diagram of the heavy-fermion superconductor CeRhIn₅. One of the many exotic properties of this material is that the conduction electrons of CeRhIn₅ turn out to be quite heavy and therefore move much slower than electrons in typical metals like copper. What is even more remarkable is that they live on the edge of two quantum states which are usually mutually exclusive. The duality of their nature is expressed in a localized versus itinerant behavior that has been experimentally observed in their antiferromagnetic versus superconducting attributes. Understanding this very anomalous electronic behaviour is one of the grand challenges of strongly correlated electron physics.

Analysis of the CeRhIn₅ phase transitions have been visually studied before using 2D plots. Here, using CINT's visualization capabilities the scant experimental set of phase transition points were integrated into a single 3D visual model to explore interactively the phase diagram. We interpolated and extrapolated the experimental data to create smooth and continuous surface boundaries that are consistent with the laws of thermodynamics and the theory of quantum phase transitions. These surfaces allowed us to study the phase transitions and in particular the interactions of the antiferromagnetic and superconducting phases.

It has been argued that the observed electronic duality is linked to the existence of a line of quantum critical points in this material. A quantum critical point is the end point of a phase transition line that ends at absolute zero temperature (quantum) and can, for example, be tuned continuously by an external parameter like pressure, chemical doping or magnetic field. Unlike in classical phase transitions, the physical properties near a quantum critical point are governed by quantum fluctuations, which can extend far above absolute zero temperature and result in novel physical properties. Since quantum critical points have been argued to play an important role in the high-temperature copper-oxide superconductors, it is thought that a better understanding of the nature of these quantum critical points may lead to new classes of superconductors with higher superconducting transition temperatures, maybe even as high as room temperature. The great advantage of studying these phenomena in the heavy-fermion system CeRhIn₅ lies in the facile tunability and accessibility of external parameters like pressure, magnetic field and chemical doping.

[sidebar: Measurements in an external magnetic field reveal the dual nature of cerium's single 4f electron and its role in creating the coexisting phase of antiferromagnetism and superconductivity. The first sidebar figure shows the pressure-field-temperature phase diagram for CeRhIn₅ with its many different quantum phases.

Regions of normal metal (N), local-moment antiferromagnetism (AFM), and superconductivity (SC) are separated by phase boundaries. The remarkable quantum critical region where AFM and SC coexist is of great interest and intensely studied. The interpretation is that as pressure increases the 4f electron becomes more itinerant and the superconducting dome grows at the expense of antiferromagnetically ordered local moments. Consequently, the nature of field-tuned quantum criticality observed between pressures 1.7 GPa and 2.2 GPa can be understood as a multi-critical line where the Fermi surface of the conduction electrons reconstructs and magnetic quantum fluctuations diverge. The consequences of these divergent quantum fluctuations can be seen at temperatures as high as 5 K with a wedge-like shape in the color map of the resistivity, even at zero-magnetic field.



Sidebar figures captions: The phase diagram of CeRhIn₅ as function of the temperature T (K= Kelvin), pressure P (GPa=Giga-Pascal) and magnetic field B (T=Tesla). N stands for “normal phase”, AFM for “antiferromagnetic” phase, and “SC” for the superconducting phase. The color bar gives the resistivity (in units of $\mu\Omega\text{-cm}$) that goes to zero as the SC region is approached. The cubic and spherical points are the experimentally measured data

points extracted from the jumps in the specific heat, and the surfaces are created using interpolation. The “white surface” separates the antiferromagnetic phase from the normal phase at high temperature. The pink surface surrounds the superconducting region at the lower temperature region. The white surface penetrates into the pink surface. The common region between the white and the pink surfaces, inside the pink region, defines the coexistence region of the AFM and SC phases. The AFM transition temperature decreases with pressure. At T=0 K, the system undergoes a transition as a function of pressure which characterizes the quantum critical region.]

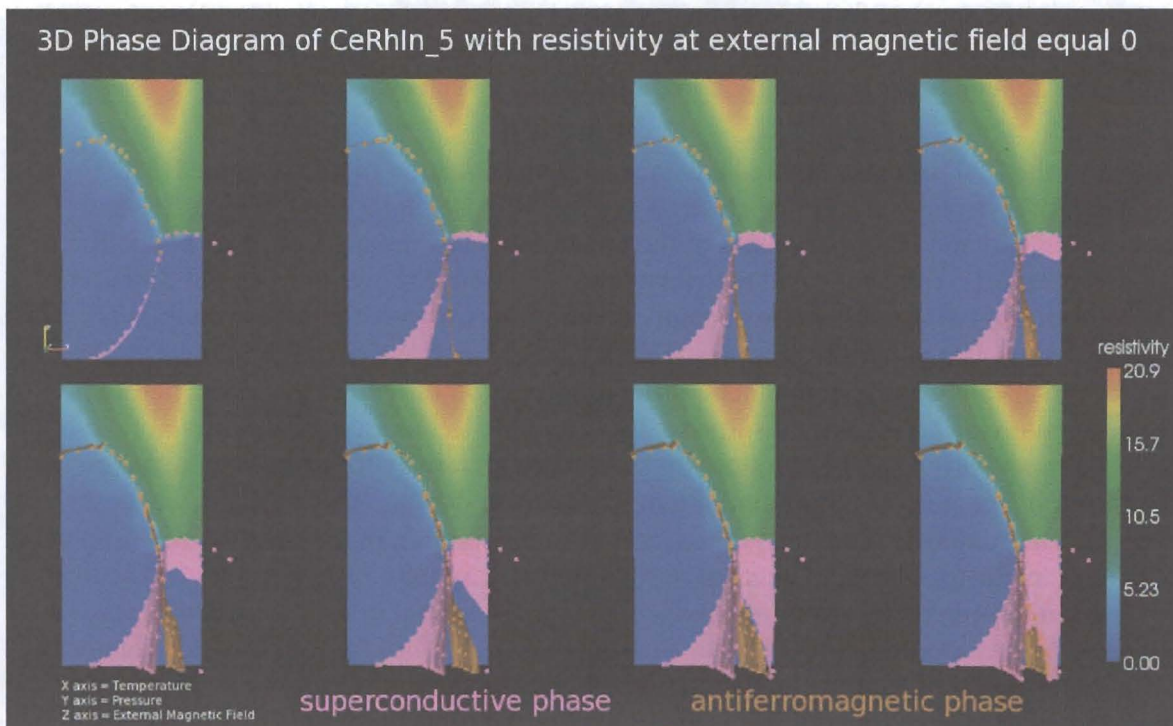


Figure Caption: This comparative 3D visualization contains several elements. The phase transition surfaces are bounded at $z=0$, that means zero magnetic field, by a plane colored by resistivity ($\mu\Omega\text{-cm}$) versus pressure and temperature. The origin is in the bottom left hand corner of each image. The image series progresses from left to right and top to bottom and shows various outputs of the clip visualization operation that removes the data from some side of a (clip) plane. As the clip plane moves through the volume of the phase diagram, one can see how the superconducting (pink) and antiferromagnetic (orange) phase boundaries intersect as the external magnetic field increases in steps of 1.1 T.

NMR spectroscopy of nano-sized droplets in the heavy-fermion system CeCoIn₅

Nuclear magnetic resonance (NMR) is a mature and powerful technique for probing the electronic state of matter by measuring the interaction between the spin of the atomic nucleus and the spin of electrons. Since the quantum mechanical interaction between the

nucleus and electron is well understood, it offers a unique and direct probe of the electronic configuration of matter at the atomic level. In collaboration with Dr. Nicholas Curro (UC Davis) and Dr. Ricardo Urbano (Los Alamos), we studied the fundamental interactions and ordering phases of the strongly correlated heavy-fermion system CeCoIn₅ doped with cadmium by using advanced visualization approaches to their multi-dimensional NMR spectra. Standard analysis methods of NMR experiments, which integrates out most of the multi-dimensional information of the NMR spectrum, reveal the existence of antiferromagnetic and superconducting order in CeCoIn₅ when doped with a few percent of cadmium. We wondered if these low-temperature quantum phases shouldn't leave a clear signature in the spectral function of the measured magnetization as well, and maybe even offer a more distinct identification of the onset of long-range and short-range antiferromagnetic order in strongly correlated electron systems.

For the first time, we applied advanced 3D visualization methods to the NMR spectrum of a strongly correlated electron system. We used ParaView to visualize and explore the real and imaginary parts of the measured NMR magnetization as a function of temperature, echo frequency and recovery time. The figure shows the spectral function of CeCoIn₅ doped with roughly one percent of cadmium (Cd) substituting for indium (In). The obtained result is much more complex than we anticipated. We can clearly identify the onset of long-range antiferromagnetic order as a function of temperature long before its sharp signature at 2.8 K. To our surprise, we were able to identify one additional feature in the spectrum at around 2.1 K. Follow-up studies are underway to determine the nature of this spectral signature as a function of temperature and doping. This newly discovered spectral feature may be due to an inhomogeneous distribution of nanoscale-sized droplets of cadmium clusters, or to an unequal occupation of cadmium on non-equivalent lattice sites of indium (there are two un-equivalent symmetry sites), or to the onset of a second antiferromagnetic ordering phase with a uniquely different nesting wave vector connecting different regions of electrons on the complex Fermi surfaces of CeCoIn₅. At the current point, we cannot even rule out if it is an artefact of the superfluid transition of the cooling medium helium. At the moment all these possibilities are being explored further.

Visualization has enabled us to see the full content of the NMR spectrum and allowed us to explore in more detail the consequences of the formation of nano-sized cadmium droplets in the bulk of the heavy-fermion system CeCoIn₅ when doped with cadmium. There is mounting evidence that the dopant cadmium is neither randomly nor uniformly substituting for indium and more research is required now that we know where to look for its signatures in the NMR spectrum.

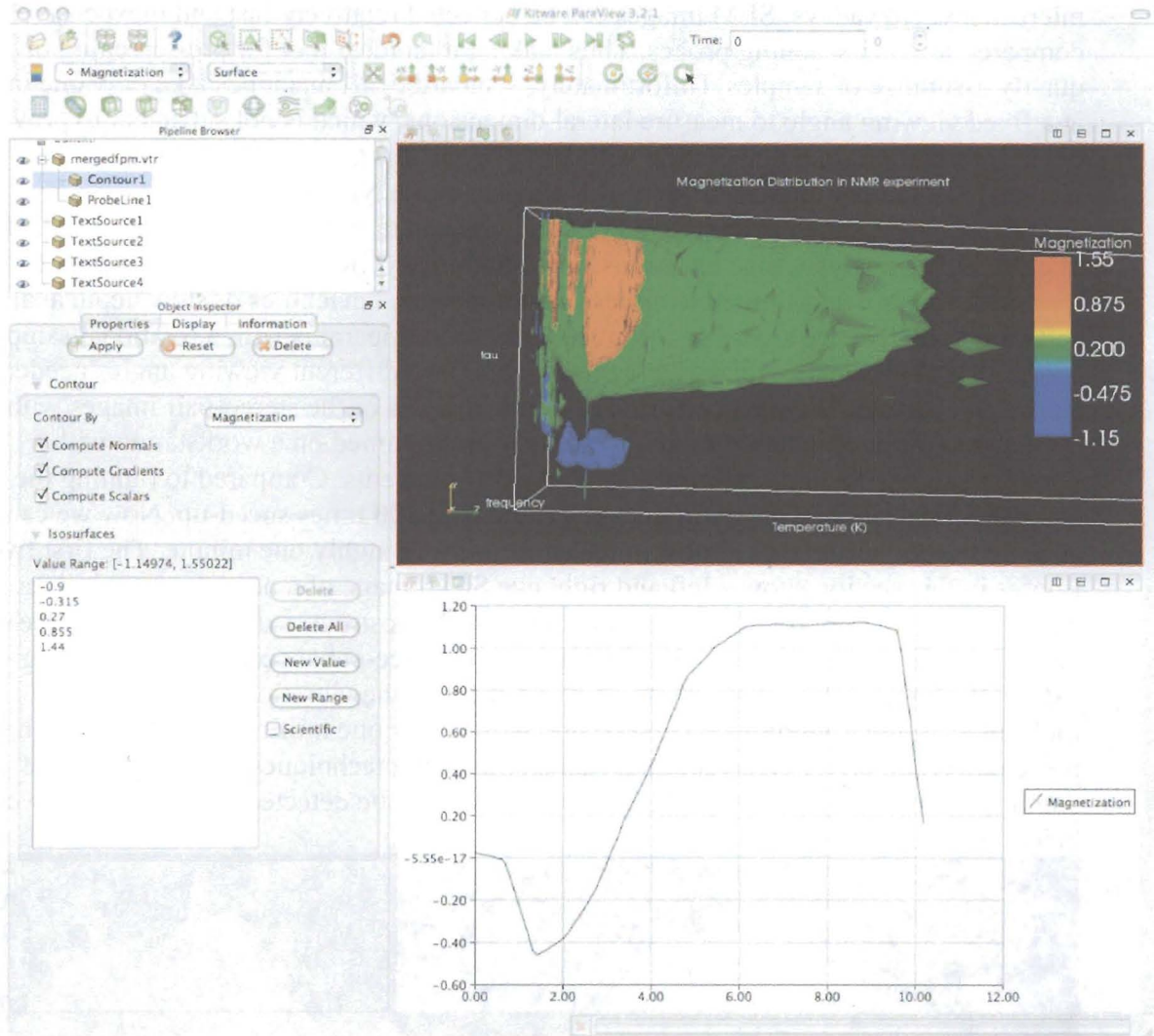


Figure caption: In this figure, we used ParaView to create a 3D visualization and 2D plot that present the magnetization distribution in an NMR experiment. The 3D window shows a collection of 3D contours of magnetization (-0.9 (blue), -0.315, 0.27 (green), 0.855 (orange) and 1.44). The X axis is normalized frequency, the Y axis is the natural logarithm of recovery time τ in micro-seconds, and the Z axis is temperature in Kelvin. The plot window below shows the magnetization as a function of $\log \tau$ at fixed temperature ($T=2.8$ K) and at zero frequency sampling along the probe line shown as a vertical line on the left side in the 3D view.

Depth map analysis with scanning electron microscopy

Scanning electron microscopy (SEM) is a standard imaging tool all the way down to the micro- and nanometer scale for objects with a conducting surface. The invention of the powerful technique of electron microscopy was finally honored when Ernst Ruska was awarded the Nobel Prize in Physics in 1986 for his fundamental work in electron optics and

microscopy. Nowadays, SEM images can be collected relatively fast and inexpensively compared to other scanning probes. Thus making it an ideal tool for pre-screening or quality assurance of samples. Unfortunately, standard SEM machines take only one image at a fixed viewing angle to measure lateral dimensions, which is not sufficient to provide depth information. In collaboration with Dave Modl, Dr. Laura Monroe at Los Alamos National Laboratory and Dr. Elshan Akhadov at Sandia National Laboratory we developed an efficient approach to extract depth or height information from a stereo-pair of SEM images. Depth analysis, also known as stereogrammetry, in combination with SEM has a long tradition, but was limited to either custom-designed machines or slow depth analysis software. At CINT we are using a conventional SEM apparatus with a rotational sample holder that allows taking images at a minimum of two different viewing angles needed for stereo-pair images. We then performed a depth analysis of the stereo-pair images with a normalized cross-correlation function analyzer programmed on a workstation with a graphics processing unit featuring 128 processing elements. Compared to running the same algorithm on a single workstation we saw more than 100 times speed-up. Now we can analyze stereo-pair images almost in real-time within roughly one minute. The first two figures in this section show a left and right eye SEM image of a nanostructured silver particle that is six micrometer along the long axis. Nanostructured silver particles are of great technological interest for developing better surface-enhanced Raman scattering (SERS) techniques, which enable the measurement of the vibrational spectrum of molecules, or the fingerprint of a molecule, with nearly one million times higher signal to noise ratio compared to conventional Raman scattering techniques. Thus even tiniest amounts of molecules, even single molecules, can now be detected that previously were below the detection threshold.

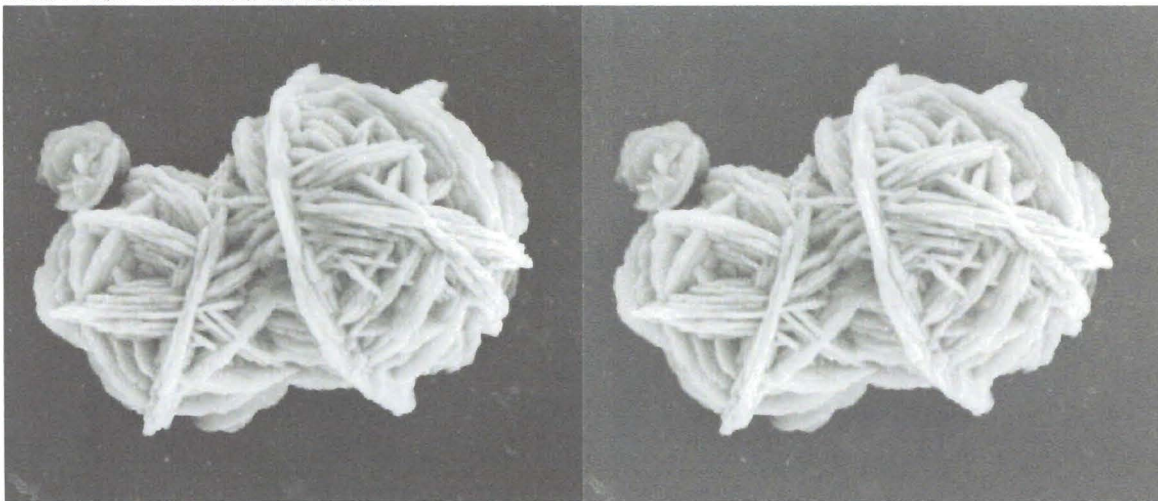


Figure caption: Left and right eye images of micro-meter-sized silver particle.

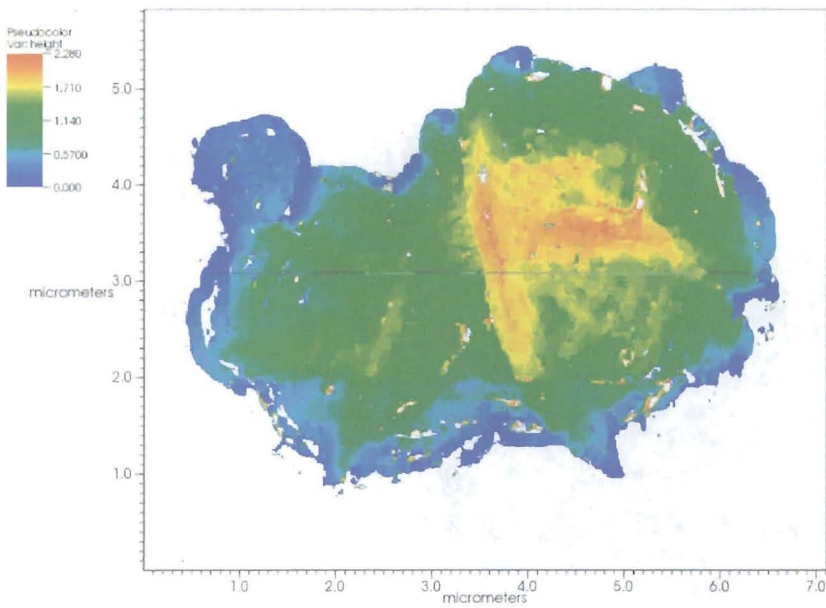


Figure caption. Contour plot of depth (height) map of silver particle with horizontal probeline.

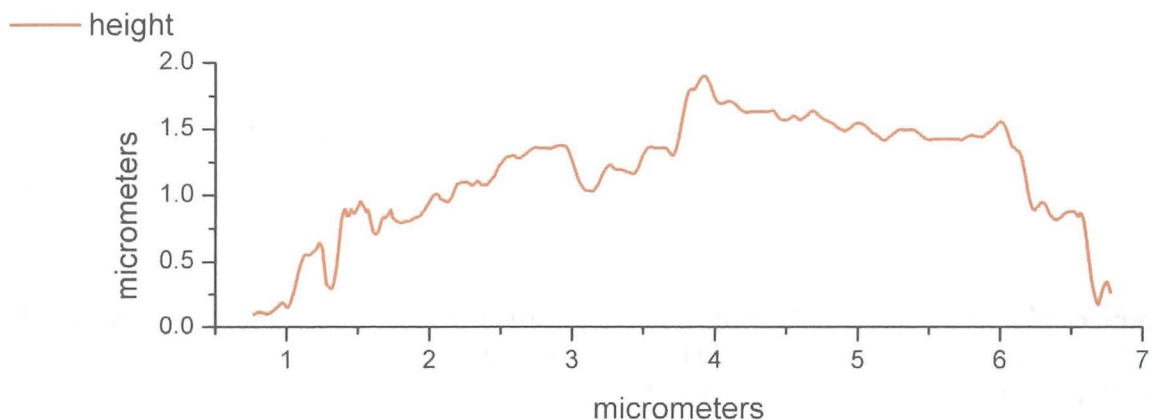


Figure caption. Quantitative height analysis along probeline shown in contour plot.

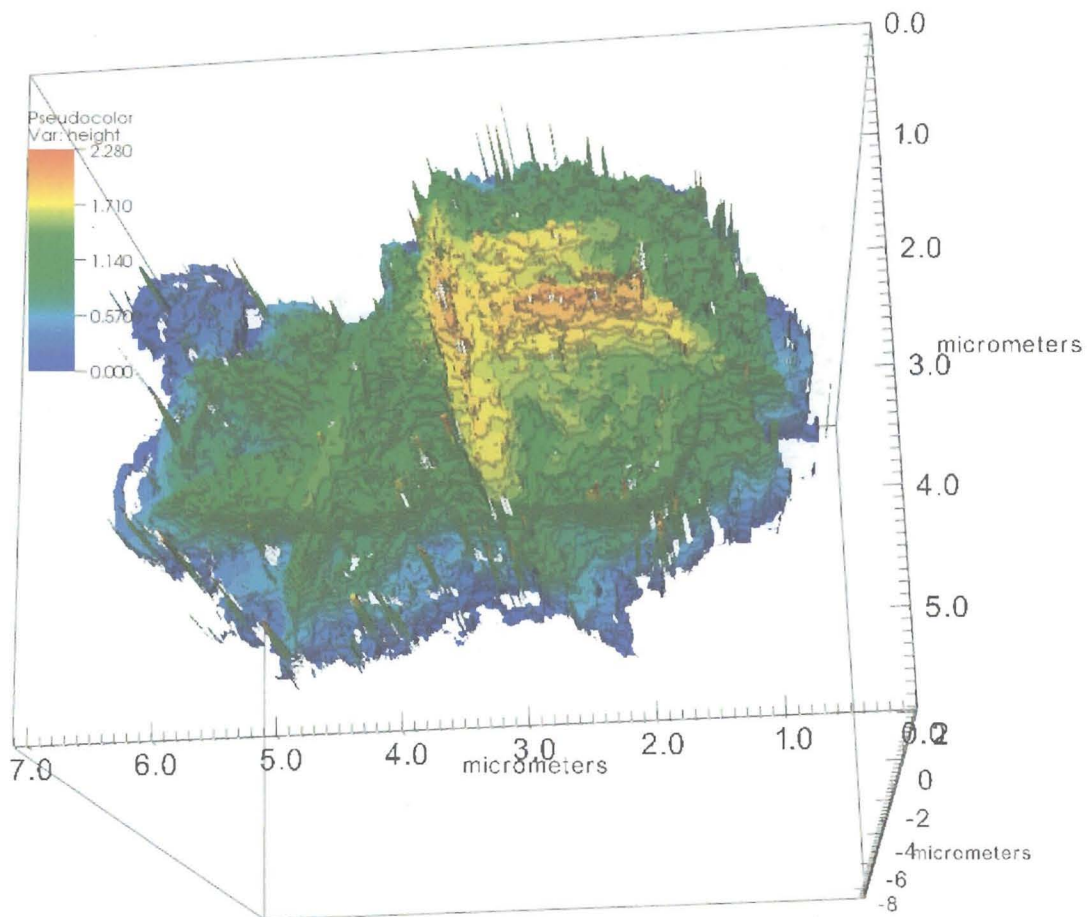


Figure caption: Reconstructed 3D image of nanostructured silver particle with color-coded height information using the freely available visualization package VisIt from Lawrence Livermore National Laboratory (<https://wci.llnl.gov/codes/visit>).

Further reading

1. “Interplay of electron–lattice interactions and superconductivity in $\text{Bi}_2\text{Sr}_2\text{CaCu}_2\text{O}_8$ ”: Jinho Lee, K. Fujita, K. McElroy, J. A. Slezak, M. Wang, Y. Aiura, H. Bando, M. Ishikado, T. Masui, J.-X. Zhu, A. V. Balatsky, H. Eisaki, S. Uchida and J. C. Davis, *Nature* **442**, 546 (2006).

2. “Electronic duality in strongly correlated matter”: T. Park, M. J. Graf, L. Boulaevskii, J. L. Sarrao, and J. D. Thompson, Proc. Nat. Acad. Sci. **105**, 6825 (2008).

Contributors. Dave Modl, LANL; Dr. Laura Monroe, LANL; Dr. Elshan Akhadov, SNL; Dr. Scott Bardenhagen, LANL.

Acknowledgements. Work at Los Alamos National Laboratory was performed under the auspices of the US Department of Energy, Office of Science.

Cover Image

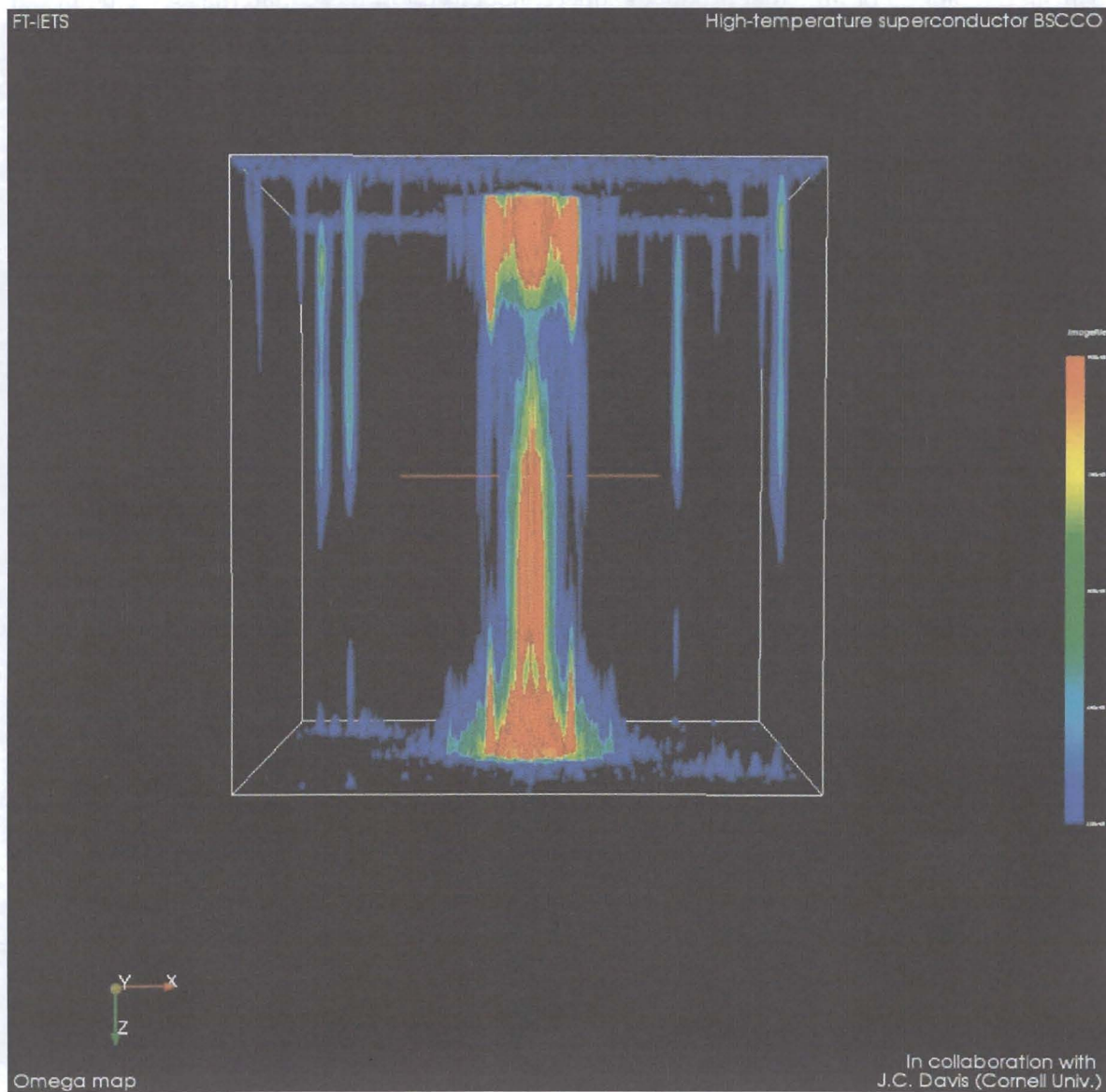


Figure caption: Scanning Tunnelling Microscopy enables the measurement of inelastic processes at the nanoscale. In this example, we show the processed inelastic tunnelling data taken on the $\text{Bi}_2\text{Sr}_2\text{CaCu}_2\text{O}_8$ superconductor. In a first step, the inelastic signal was acquired over the given field of view as a function of tunneling voltage V . Then a set of images was taken for a range of bias voltages and subsequently was Fourier transformed (FT) to obtain the energy dispersion in momentum space, due to inelastic scattering of electrons. The two coordinates in the x - y plane are FT momenta k_x , k_y and the third, vertical dimension is the tunneling bias V . The STM data is a function of all three coordinates (k_x , k_y , V). The cover page shows the FT STM image as a 3D still image. We used our visualization capabilities at CINT to analyze and render the data in stereo. This

image encodes the dispersion (energy vs momentum) of the inelastic scattering process of electrons in high-temperature copper-oxide superconductors that might be related to the pairing interaction or glue that produces superconductivity in these materials. We point out that the corresponding real space data ubiquitously show the nanoscale inhomogeneity in these materials.